Reliable Automatic Camera-Laser Calibration

Abdallah Kassir and Thierry Peynot
ARC Centre of Excellence for Autonomous Systems
Australian Centre for Field Robotics
The University of Sydney, NSW 2006, Australia
{a.kassir@acfr.usyd.edu.au, tpeynot@acfr.usyd.edu.au}

Abstract

Camera-laser calibration is necessary for many robotics and computer vision applications. However, existing calibration toolboxes still require laborious effort from the operator in order to achieve reliable and accurate results. This paper proposes algorithms that augment two existing trustful calibration methods with an automatic extraction of the calibration object from the sensor data. The result is a complete procedure that allows for automatic camera-laser calibration. The first stage of the procedure is automatic camera calibration which is useful in its own right for many applications. The chessboard extraction algorithm it provides is shown to outperform openly available techniques. The second stage completes the procedure by providing automatic camera-laser calibration. The procedure has been verified by extensive experimental tests with the proposed algorithms providing a major reduction in time required from an operator in comparison to manual methods.

1 Introduction

Despite being extensively carried out across different robotics and computer vision applications, camera-laser calibration remains a challenging problem. Existing calibration toolboxes still require laborious effort from the operator in order to achieve reliable and accurate results. This paper presents an automatic, robust and complete procedure for the calibration of a perspective camera with a 2D laser range finder. The goal of the procedure is to find accurate estimates of the intrinsic parameters of the camera and the rigid transformation between the camera and the laser under the assumption of known intrinsic parameters of the laser. The work has been divided into two stages: automatic camera calibration and automatic extrinsic camera-laser calibration. Rather than pursue self-calibration methods, the paper presents algorithms that automate two existing trustful calibration methods which rely on observing a calibration object and which jointly achieve complete camera-laser calibration: Bouguet's Camera Calibration Toolbox [Bouguet, 2010] and Zhang and Pless's extrinsic camera-laser calibration technique [Zhang and Pless, 2004b]. To use these techniques, the operator is required to obtain a calibration dataset, which is a set of synchronised pairs of images and laser scans, containing a chessboard and taken from different poses. The chessboard acts as the calibration object and the size of its squares needs to be measured. For the camera calibration, the corners of the chessboard squares need to be extracted from the images. In the toolbox, this is attained by the outer corners being selected manually. The toolbox outputs the camera intrinsic parameters as well as the rigid transformation from the camera to the chessboard for each image. The transformation is necessary for the camera-laser calibration technique cited above. The camera-laser calibration then uses the points originating from the chessboard which appear in the laser scans to find the camera-to-laser rigid transformation. Typically, these points have to be extracted manually. In both cases, the extraction process is the key time consuming task for the operator. Aimed at automating the entire procedure, two algorithms are presented: the first automatically extracts the chessboard corners from each image and the second extracts the chessboard points from the laser scans. With the aid of these algorithms, the required operator time is reduced to what is needed for acquiring the calibration dataset and measuring the size of the chessboard squares. The procedure has been verified by extensive experimental tests. The automatic chessboard extraction algorithm is shown to produce improved results over existing methods. The automatic camera-laser calibration method demonstrates accuracy while significantly reducing operator time when compared to manual methods.

Section 2 details the proposed method for the automatic calibration of the camera alone. It first examines

existing automatic camera calibration techniques, then explains the proposed chessboard extraction algorithm. Section 3 describes the automatic camera-laser transformation estimation method. A concise survey is presented followed by the suggested chessboard extraction from laser algorithm. Finally, Section 4 draws conclusions and directions for future work.

2 Automatic Camera Calibration

2.1 Existing Methods

Camera self-calibration, which is a calibration process that does not require an explicit calibration object, has been studied extensively by researchers [Faugeras *et al.*, 1992; Hartley, 1994; Luong and Faugeras, 1997; Pollefeys, 1999]. However, a fully automatic version of self-calibration is yet to become reliable due to the point correspondence problem and restrictive assumptions [Bougnoux, 1998; Remondino and Fraser, 2006]. Moreover, self-calibration does not provide the extrinsic parameters required for the extrinsic camera-laser calibration.

Meanwhile, numerous algorithms for automatically extracting the chessboard grid from an image exist with varying degrees of automation and reliability. OpenCV offers an automatic extraction function using Vezhnevets's algorithm [Vezhnevets, 2010]. Rufli [Rufli *et al.*, 2008] suggests an improved version of the algorithm which is provided in the OCamCalib Matlab Toolbox [Scaramuzza, 2009]. The two algorithms rely on detecting quadrangles obtained through the erosion of the binarised image. Since they rely on the separation of the chessboard quadrangles, they are sensitive to image blur. Moreover, they do not automatically deal with cases where the full grid was not found.

Another group of algorithms relies on detecting Harris corners or feature points which are then arranged into a grid. Some of these algorithms apply a classifier to filter out non-chessboard corners, such as [Ha, 2009; Zhou and Fang, 2010; Wang *et al.*, 2010] while others do not, such as [Douskos, 2008]. Without the use of a classifier or filter, performance is greatly degraded by clutter. It has been noticed that existing algorithms are complementary in some sense. For instance, the chessboard corner filter in [Ha, 2007] could aid the algorithm suggested in [Douskos, 2008]. This complementariness was exploited in this work to produce a robust extraction algorithm.

DLR CalDe [Strobl *et al.*, 2009] is another piece of software which offers automatic chessboard corner detection; it requires a chessboard with three solid circles at its centre. In some cases, it also requires erroneous points to manually be removed. Algorithms in [Wang *et al.*, 2010; Zhou and Fang, 2010; de la Escalera and Armingol, 2010] rely on line fitting or the Hough transform. It is suspected that such algorithms will be greatly affected by nonlinear distortion. The algorithm in [Ha, 2009] is an improved version of the original algorithm described in [Ha, 2007]. The latter introduced an interesting chessboard corner filter. Unfortunately, neither this algorithm nor any of the previously mentioned discuss the effect of image conditions, such as scale and illumination for example, on tools used such as the Harris corner finder or the Hough transform. On the other hand, the algorithm introduced below introduces feedback which deals with the problem of scale. It also suggests a means to automatically select a region for the chessboard corner filter.

2.2 The Algorithm

As with any image feature extraction algorithm, the performance of an automatic chessboard extraction algorithm needs to be examined under different conditions. If the issues associated with the change in conditions are carefully addressed and the algorithm is tested with a large number of images from different datasets, a reliable algorithm can be obtained. The algorithm introduced below is focused on addressing the following issues:

- Illumination invariance
- Scale invariance
- Clutter immunity
- Minimising the number of user tuned parameters

By addressing these issues, the algorithm's capability supersedes that of any of the openly available existing algorithms as summarised in Table 1. Our algorithm manages to encompass necessary features missed by existing algorithms. This is achieved mainly through the careful choice of a combination of detection tools in addition to introducing feedback.

The steps of the algorithm are listed below. The first step is adaptive contrast enhancement which is detailed in Section 2.3. This is followed by a Harris corner finder using three different window sizes. For each size, the Harris corners are passed through a chessboard corner filter similar to that suggested in [Ha, 2007]. Out of the sets of corners obtained for each window size, the one with largest number of corners remaining after the filter is chosen for the next step. This process is explained in Section 2.4. This set of candidate corners is then arranged into a grid. The grid arrangement step is comparable to that used by [Douskos, 2008]. The grid is then filtered for outliers and missing corners are linearly interpolated. Grid extraction is described in Section 2.6. The grid is finally fed into Bouguet's calibration optimisation routine. In the following sections, the steps of the algorithm will be described with further detail, highlight-

Table 1: Comparison of features offered with existing toolboxes

	Scale invariance	Lightness invariance	Clutter immunity	Distortion invariance	Limited use of thresholds
OCamCalib	✓	✓	✘	✓	✓
FAUCCAL	✘	✓	✘	✓	✓
OpenCV	✓	✘	✘	✓	✓
Ha's Method	✘	✓	✓	✘	✘
Our Algorithm	✓	✓	✓	✓	✓

ing the approach taken to solve each of the issues listed earlier.

Automatic Chessboard Extraction Algorithm

1. Apply adaptive contrast enhancement.
2. Choose three different window sizes for the Harris corner finder.
3. For each window size, apply the corner finder then run the detected corners through the chessboard corner filter.
4. Choose the largest set of corners for the next step.
5. Arrange the corners into a grid.
6. Remove grid outliers and interpolate missing corners.
7. Run Bouguet's calibration routine.

2.3 Adaptive Contrast Enhancement

An image taken under poor lighting conditions lacks high contrast within the chessboard and hence will decline the quality of the Harris transform, which relies on intensity differences. Nevertheless, the intensity difference between the chessboard's black and white squares can be exploited through adaptive contrast enhancement. Global contrast enhancement investigates the properties of an image as a whole and then applies the same intensity transformation for all pixels, while adaptive contrast enhancement looks at the local properties of the image. The version of adaptive contrast enhancement used here adjusts the intensity of each pixel based on the mean and standard deviation of the intensities inside a window around that pixel. Taking into account different possible image sizes, the window size is chosen proportional to the image size. Adaptive contrast enhancement achieves the required illumination invariance. After the Harris transform of an image is obtained, a thresholding mechanism is utilized to obtain blobs around the corners. The centroids of the blobs are extracted as pixels representing the Harris corners.

2.4 Harris Transform Window Size

The window size chosen for the Harris transform affects its performance. The window has to be large enough in order to detect a corner in the region as opposed to an edge. However, if the window size becomes comparable to the size of the chessboard squares in the image, adjacent corners can get fused together. Therefore, choosing the right window size is essential for the successful extraction of the chessboard corners. In order for the algorithm to be able to automatically select the appropriate window size, it needs a metric or a reward. Once that is available, it can simply choose the window size with the highest reward. The proposed reward is the number of corners that pass the chessboard corner filter. This introduces feedback into the algorithm. To the best of our knowledge, none of the existing algorithms employ this feedback to improve the performance of the Harris corner detector. This feature of the algorithm introduces reliable scale invariance.

2.5 Chessboard Corner Filter

Constructing the chessboard grid crudely from the Harris corners can result in failure on cluttered images. The chessboard corner filter is the key to clutter immunity. It provides a distinctive advantage over methods that do not employ such a filter, e.g. [Vezhnevets, 2010; Rufli *et al.*, 2008; Douskos, 2008; Strobl *et al.*, 2009]. The design of this filter is based on the method described by Ha [Ha, 2007]. The filter classifies corners using two criteria:

1. A chessboard corner lies at the intersection of two edges.
2. The area around the corner consists of alternating white and black or high and low intensity regions corresponding to the chessboard squares.

The chessboard corner filter serves to classify corners either as part of a chessboard or as a corner in the background. The filter checks the properties of the region around the corner pixel. The filter in [Ha, 2007] relies on user-selected parameters to define the test region. To achieve the goal of minimising the number of

user-defined parameters, our algorithm automatically selects the region by expanding a square window until it approaches neighbouring Harris corners. The main assumption is that most chessboard corners were successfully detected by the Harris corner finder and that no Harris corners other than those corners exist inside the chessboard area. Based on this assumption, the region chosen for the filter is the largest square region centred at the corner not including any other corners. Fig. 1 shows the selected region marked in yellow for a certain corner.

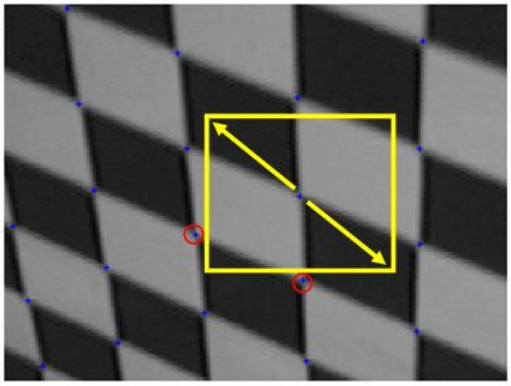

Figure 1: Automatic selection of test region. A square region (yellow box) centred at a Harris corner is expanded until it hits other Harris corners (red circles).

2.6 Grid Extraction

Grid extraction is a critical step in the algorithm. The input to this step is the candidate corners which passed the filter. The output of this step is an array of corners whose rows and columns correspond to the rows and columns of the chessboard grid. The grid extraction algorithm used here is adapted from [Douskos, 2008]. A feature characteristic of a chessboard pattern is that every non-diagonal pair of adjacent corners is connected together by an edge that has a constant gradient direction. In other words, along the connecting edge, one side is white and the other side is black. The gradient direction can easily be obtained from the Sobel edge transform. Given any chessboard corner, the other four adjacent corners can be found using the criteria mentioned. The starting point is chosen as the candidate corner which is closest to the mean of the candidate corners' (u, v) coordinates. The steps of the grid arrangement algorithm are listed below. Grid arrangement corresponds to step 5 of the automatic chessboard extraction algorithm.

Grid Arrangement Algorithm

1. Get the corner closest to the mean of the candidate corners' (u, v) coordinates.
2. Place this corner in the middle of a large empty array. This corner becomes the current corner.
3. From the current corner, obtain the nearest 8 corners, in Euclidean distance sense, from the list of candidate corners.
4. Sweep the region in the edge image around the current corner to obtain the direction of the four peaks.
5. For each peak, choose the corner, out of the nearest 8, that occurs along the direction corresponding to the peak. These should be the adjacent corners.
6. Arrange the adjacent corners according to their angle, to be placed in the array around the current corner. If the current corner is the first corner in the array, then choose a random reference direction. Otherwise, look for corners already existing on the array and match to make the direction consistent.
7. If a match is found or if the current corner is the first corner in the array, place the adjacent corners in the array, mark the current corner as expanded and mark the adjacent corners as unexpanded; otherwise, if no match is found, remove the current corner from the array.
8. If there still are unexpanded corners, move on to the next unexpanded corner which becomes the current corner and go to step 3. Else, end.

Corners not belonging to the chessboard might pass the filter and erroneously tag to the grid during grid arrangement. Therefore, starting from the border lines, lines are removed if the number of corners existing is less than half the total length of that line. This is applied continuously until no more lines are removed. Once the grid is filtered, the remaining lines are checked for gaps. When a gap is located, the position of the corresponding point is interpolated. A line is fit, in a least squares sense, to the column and row to which it belongs. The point is then estimated to be at the intersection of the two lines. Finally, the sub-pixel corner finder provided by Bouguet is used to find the sub-pixel location of all the corners in the extracted grid. The grid is then ready to be fed into the calibration routine of Bouguet's toolbox which runs an optimisation to retrieve the camera calibration parameters.

Results and comparison of the extraction algorithm in addition to a comparison of calibration results are shown in Section 2.7.

2.7 Experimental Results

The automatic chessboard extraction algorithm has been tested on more than 200 images acquired by different cameras under different scale, lighting, clutter and distortion conditions. Fig. 2 illustrates scale invariance

where the ratio of the size of squares between the images is approximately 6:1. The image on the right also shows the immunity against clutter. Fig. 3 illustrates the algorithm's performance under distortion.

For the purpose of comparison, we have chosen 99 images from 6 different datasets. The test datasets include all the sample images provided by the toolboxes listed in Table 2 in addition to three of our own. The images were sorted into categories according to their scale, illumination, clutter and distortion properties. Table 2 displays the comparison with the other toolboxes. The values in the table are the percentage of the images from which the toolboxes extracted a grid which is useful for calibration. The values in the table show a significant advantage for our algorithm in regards to illumination conditions and scale. This can be attributed to the feedback in the algorithm. As mentioned in Section 2.1, existing methods fail to address the issue of scale. This is confirmed in the results as the table shows extremely low scores for images with poor scale. Also evident from the table is the improvement in performance under clutter compared to FAUCCAL due to the use of a chessboard corner filter. Another interesting observation is the excellent performance of our algorithm under distortion.

Table 3 shows a comparison of the calibration results obtained via both manual and automatic extraction using Bouguet's sample dataset and another from the Marulan datasets [Peynot *et al.*, 2010]. The results show no degradation in the quality of calibration for Bouguet's dataset and a minute effect on the results for the Marulan dataset. In either case, the RMS pixel reprojection error was below 0.2 pixel.

The automatic extraction of the chessboard grid has a reasonable runtime of 9 seconds per 1.3 megapixel image on a standard 2.1GHz dual-core PC. Manual extraction achieved by an operator has been estimated to take an average of 20 seconds per image. Consequently, by using our automatic extraction, at least 10 minutes of demanding operator time are substituted by 4.5 minutes of computer time for a 30-image dataset.

By augmenting the automatic chessboard detection algorithm to Bouguet's toolbox, automatic camera calibration is achieved. Besides the acquisition of the calibration images, the only required effort from the operator is to provide the toolbox with the size of the squares. Contrary to some existing methods, this automatic extraction does not require the number of squares along each dimension of the chessboard. However, if the size of the chessboard squares is not the same along each dimension, the chessboard direction should be consistent throughout the dataset. Automatic camera calibration can be useful in its own right for many applications. Nevertheless, it is a necessary step towards automating camera-laser calibration. Section 3 discusses the second step of the procedure.

3 Automatic Camera-Laser Calibration

3.1 Existing Methods

Most of the work in the area of automating camera-laser calibration focuses on self-calibration. Zhang and Pless [Zhang and Pless, 2004a] presented a method for the self-calibration of a camera with a laser range finder. The method uses motion information from the sensors and epipolar constraints to optimise the calibration, all of which are heavily reliant on establishing point correspondences. Moreover, the results in the paper are not comprehensive enough to establish confidence. Scaramuzza [Scaramuzza *et al.*, 2007] presents another self-calibration method using a 3D laser range finder where the operator is required to manually select corresponding features. Self-calibration methods still require point correspondence establishment from the sensor data and lack the required accuracy for most applications in robotics. Therefore, we have chosen to automate the manual extrinsic camera-laser calibration method by Zhang and Pless [Zhang and Pless, 2004b].

3.2 The Algorithm

Through a similar approach to Section 2, the algorithm here is designed for the automatic extraction of the chessboard from the 2D laser dataset. A single 2D laser scan gives very little information about the location of the chessboard line. Much more information can be gained by the integration of information from the entire dataset. Therefore, in the algorithm described in this section, chessboard extraction is achieved by using the entire dataset to estimate the length of the chessboard in the laser scans and through the iterative refinement of the transformation estimate (Section 3.4).

The flow of the algorithm is shown in Fig. 4. The algorithm begins with straight line extraction, explained in Section 3.3. Once the straight lines are extracted, they need to be classified into chessboard or background lines. From the classified lines, an estimate of the camera-laser rigid transformation is obtained. This transformation is then further used to aid in the classification. Iteratively, the transformation is refined until the same lines are reselected indicating convergence of the classification. At this point, the final calculation of the camera-laser transformation is performed.

3.3 Straight Line Extraction

Many algorithms exist for extracting straight lines from 2D laser scans. [Nguyen *et al.*, 2007] contains an extensive survey of existing line extraction algorithms. Unfortunately, experimentation with these existing algorithms failed to produce satisfactory results for the purpose of our algorithm. The standard Hough transform suffers

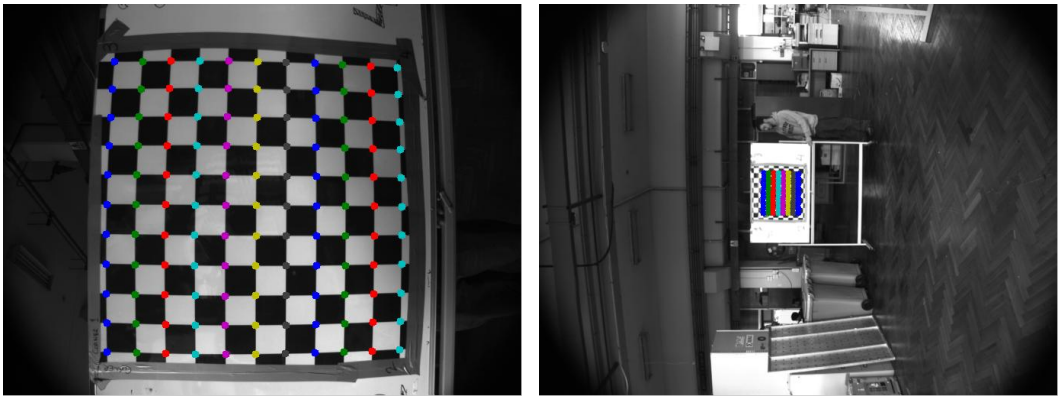

(a) (b)

Figure 2: Illustration of the algorithm's scale invariance. The size of the chessboard squares in pixels has a ratio of 6:1 between the two images. The coloured dots represent the extracted chessboard corners.

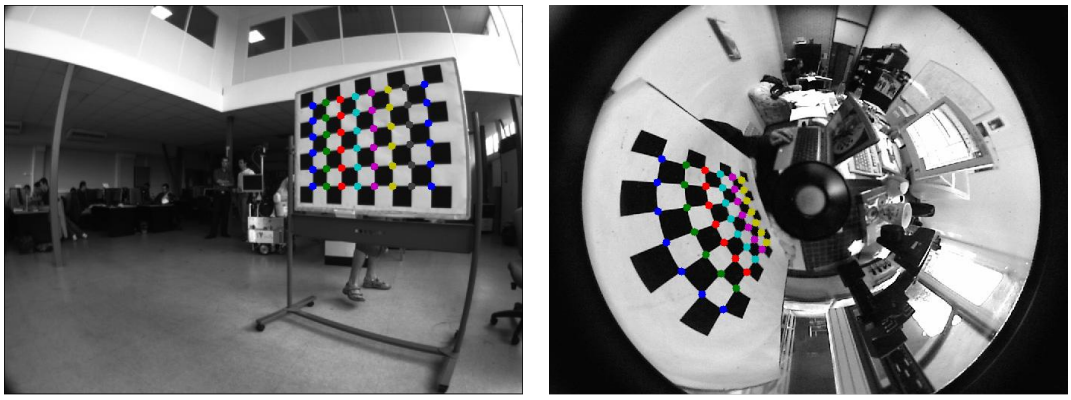

(a) (Original image from LAAS-CRNS) (b) (Original image from [Scaramuzza, 2009])

Figure 3: Illustration of the algorithm's performance under distortion. The coloured dots represent the extracted chessboard corners.

Table 2: The performance of algorithms under different image conditions. A total of 99 images from 6 different datasets were used. The images were categorised as follows: poor illumination (45 images), poor scale (chessboard covers less than 1/5 of the image)(25), cluttered (70), high distortion (36). The values in the table are the percentage of successful grid extractions from each category.

	Images with poor illumination	Images with poor scale	Images with clutter	Images with high distortion	Total
OCamCalib	4.44%	8%	67.14%	100%	56.56%
FAUCCAL	44%	0%	37.14%	72%	55.55%
OpenCV	4.44%	0%	62.85%	97.22%	55%
Our Algorithm	97.77%	96%	98.5%	100%	98.98%

Table 3: Comparison between the calibration results from the manual corner extraction and our automatic chessboard corner extraction (Error: 3 times the standard deviation).

	Bouguet's Dataset		Marulan Dataset	
	Automatic Corner Extraction	Manual Corner Extraction	Automatic Corner Extraction	Manual Corner Extraction
Focal length ± Error (in pixels)	[657.37, 657.74] ± [0.347, 0.371]	[657.39, 657.76] ± [0.346, 0.371]	[1024.74, 1022.31] ± [2.679, 2.625]	[1023.91, 1020.98] ± [3.779, 3.7]
Principal point ± Error (in pixels)	[302.98, 242.59] ± [0.706, 0.646]	[302.98, 242.61] ± [0.705, 0.645]	[659.46, 475.13] ± [3.839, 4.001]	[665.17, 476.52] ± [5.756, 6.112]
RMS Pixel Error (in pixels)	[0.126, 0.126]	[0.126, 0.126]	[0.154,0.146]	[0.141,0.118]

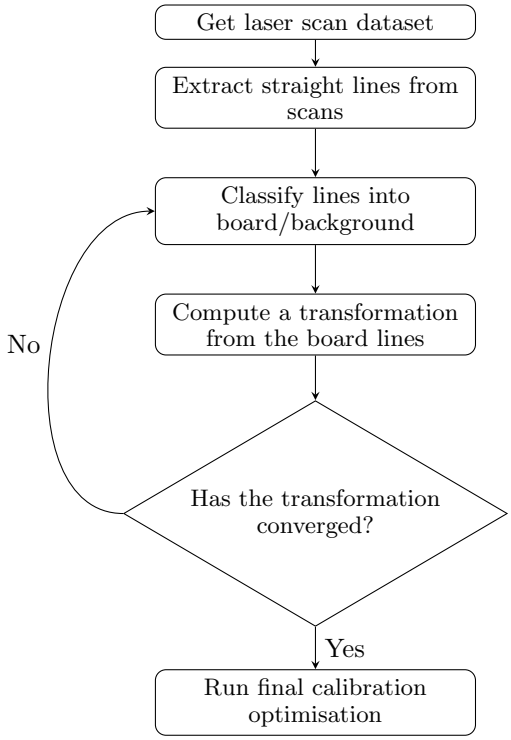

Figure 4: Algorithm for the automatic chessboard extraction from laser scans

from its dependence on the density of points which varies with the variation of the line angle in a 2D laser scan. Iterative or successive algorithms are susceptible to compromising longer lines for shorter ones. Since length is a classification metric used in subsequent steps, a different method which ensures the longest lines are extracted had to be introduced. To simplify the problem, we make the following assumptions. Occlusions or gaps are not considered and a straight line for a set of points is simply the line connecting the end points. These assumptions are reasonable for the purpose of calibration since no objects are expected to be in front of the calibration board. The selected straightness criterion for the set of points is the maximum perpendicular distance from the points to the line. The key idea of the algorithm is to recursively test every combination of two points in the scan with the straight line criterion and then recursively take out the longest line. The search has a computational complexity of $\mathcal{O}(n^2)$ for each scan with n being the number of laser points in the scan. However, the runtime is reduced by introducing a heuristic. Before the algorithm begins searching for lines, the scan is dissected at range jumps larger than a certain threshold. The heuristic also enforces the no-gap assumption.

3.4 Classification

Other lines in the laser scans, which we call background lines, might come from walls, tables and other elements in a structured environment. Thus, to distinguish those corresponding to the chessboard, the extracted lines are subject to a classification process. Three metrics are used for the classification process:

1. The frequency of occurrence.
2. The difference in length with the estimated length of the board.
3. The distance from the estimated position using the transformation estimate (once available).

Since the calibration process requires the calibration board to be moved to different poses throughout the cal-

ibration dataset, positions in the laser scan which occur quite frequently throughout the dataset are most likely to correspond to the background or irrelevant objects in the foreground. Therefore, the frequency of occurrence is the first metric used. It should be noted that the classification process is an iterative process in which the output of the classification step is used to compute a transformation estimate which is then used to refine the classification and henceforth. Unless provided by the user, the length of the board and an estimate of the camera-laser rigid transformation do not exist a priori. Therefore, for the initial iteration, the algorithm marks the line with the lowest frequency value in each scan. Its value needs to be below a certain threshold to be considered as it might be the case that all the lines in a scan have a low value, if the board does not exist in the scan for example. Using these marked lines, the length of the board is estimated and then used to remove outliers. In this way, lines which differ by more than a certain threshold from the estimated length of the board are removed. Then, a transformation estimate is obtained. For subsequent iterations, the transformation values are used to measure the distance of the lines from the estimated location of the board which is also thresholded. Collectively, and after a few iterations, the three metrics are used to successfully choose the right line from each scan.

The use of thresholds is only valid if the metrics are normalised. Otherwise, each dataset will have its own threshold. Therefore, the frequency metric is normalised over the number of scans, the length metric over the estimated length and the transformation metric over the maximum distance found. In terms of the threshold values, 0.9 was chosen for frequency and transformation. This value was chosen conservatively to ensure that only valid calibration lines are selected while sacrificing uncertain lines. A threshold value of 0.5 was chosen for length, meaning lines which differ by more than half of the estimated length of the board are discarded. The length threshold is not entirely critical since it is only used to remove extremely short or long lines.

Section 3.5 contains experimental results in regard to both the algorithm's classification performance and the quality of calibration obtained using the algorithm.

3.5 Experimental Results

Successful automatic camera-laser calibration has been performed for at least 6 different camera-laser setups. Fig. 5 shows a sample of a chessboard automatically extracted out of a laser scan. Three different calibration datasets have been chosen for the results in this section: Dataset1, Dataset2 and Dataset3. Dataset1 includes 53 scan-image pairs, all laser scans contained a board line and the camera-laser setup was stationary throughout the data acquisition. Dataset2 was sourced from the Marulan datasets [Peynot *et al.*, 2010]. It includes 74 scan-image pairs, out of which 64 contained a board line. The setup was stationary throughout the dataset. Dataset3 includes 71 scan-image pairs, out of which 50 contained a board line, yet the setup was moved a few times (about 3 times) throughout the data acquisition. Extraction results for the three datasets are summarised in Table 4 in terms of precision and recall. Note that the thresholds of the algorithm were chosen to sacrifice recall for precision. The 100% precision is desirable since including outlier data points affects the accuracy of the calibration results much more than removing some valid calibration points, especially if the dataset is large enough. Table 5 compares camera-to-laser rigid transformation estimation obtained via both manual and automatic extraction for the last two datasets. The parameter error estimates were obtained using the method described in [Peynot and Kassir, 2010]. The table shows only minute discrepancies in the transformation parameters and error.

The automatic extraction of the chessboard from the laser scans has a runtime of less than 40 seconds for a dataset of 50 laser scans. Consequently, through this algorithm, both the operator and calibration times are highly reduced.

By augmenting this automatic extraction algorithm to Zhang and Pless's calibration method, automatic extrinsic camera-laser calibration can be achieved. To ensure successful operation, the camera-laser setup should remain stationary with respect to the background, with the possible exception of a few movements, while the chessboard is relocated throughout the dataset.

Table 4: Performance of the chessboard extraction from laser scans in terms of precision and recall

	Number of scans	Precision	Recall
Dataset1	53	100%	100%
Dataset2	74	100%	100%
Dataset3	71	100%	86%

4 Conclusion

In this paper, we have proposed an automatic and complete procedure for the calibration of a camera with a laser. This work was divided into two parts. The first part attains automatic camera calibration through an algorithm that extracts chessboard corners from the images of a calibration dataset. This algorithm can be used independently for many applications merely requiring camera calibration. Given the results of the first part, the second part attains automatic extrin-

Table 5: Comparison of the camera-laser rigid transformations obtained after the automatic and manual extractions (Dataset2: 74 scan-image pairs, stationary setup, Dataset3: 71 scan-image pairs, setup moved a few times, Error: one standard deviation, Δ: translation offset, R: Euler angles)

	Dataset2		Dataset3	
	Automatic Extraction	Manual Extraction	Automatic Extraction	Manual Extraction
$\Delta\pm$ Error (in m)	[0.0002, 0.528, 0.061] $\pm$ [0.0126, 0.0044, 0.0081]	[0.0024, 0.527, 0.0607] $\pm$ [0.0077, 0.004, 0.0037]	[-0.415, 0.292, 0.037] $\pm$ [0.004, 0.004, 0.0018]	[-0.416, 0.292, 0.037] $\pm$ [0.0042, 0.0043, 0.0012]
$R\pm$ Error (in deg.)	[-0.027, 0.469, 180] $\pm$ [0.143, 0.179, 0.147]	[0, 0.405, 180] $\pm$ [0.144, 0.132, 0.155]	[4.73, 0.37, 0.44] $\pm$ [0.1, 0.053, 0.144]	[4.72, 0.39, 0.49] $\pm$ [0.104, 0.06, 0.201]
RMS Error (in m)	0.00796	0.00704	0.00755	0.00743

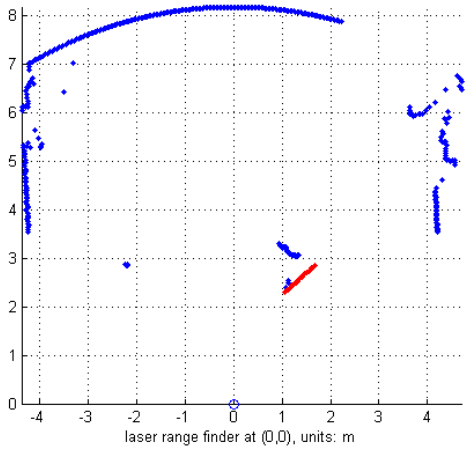

(a)

(b)

Figure 5: Sample of a successful board extraction. (a) shows the extracted points in red. (b) is the scan's corresponding image. (Scan and image from [Peynot *et al.*, 2010])

sic camera-laser calibration through an algorithm which extracts the chessboard from the laser scans of the calibration dataset. Jointly, the two algorithms provide automatic camera-laser calibration. The two Matlab toolboxes implementing these algorithms are available online at `http://www-personal.acfr.usyd.edu.au/akas9185/AutoCalib/index.html`. Extensive testing has been applied to both algorithms with results displaying significant levels of performance and accuracy especially when compared to existing automatic methods.

Future work will investigate extending the automatic camera calibration to a stereo camera pair and extending the automatic camera-laser calibration to 3D laser range finders.

Acknowledgements

This work was supported by the ARC Centre of Excellence programme, funded by the Australian Research Council (ARC) and the New South Wales State Government.

References

[Bougnoux, 1998] S. Bougnoux. From projective to euclidean space under any practical situation, a criticism of self-calibration. In *Sixth International Conference on Computer Vision*, Washington, DC, USA, 1998.

[Bouguet, 2010] J.-Y. Bouguet. Camera calibration toolbox for matlab, 2010. `http://www.vision.caltech.edu/bouguetj/calib_doc/`.

[de la Escalera and Armingol, 2010] A. de la Escalera and J. M. Armingol. Automatic chessboard detection for intrinsic and extrinsic camera parameter calibration. *Sensors*, 10(3), 2010.

[Douskos, 2008] V. Douskos. Fully automatic camera calibration using regular planar patterns. *International Archives of the Photogrammetry, Remote Sensing and Spatial Information Sciences*, XXXVII, 2008.

[Faugeras *et al.*, 1992] O. D. Faugeras, Q. T. Luong, and S. J. Maybank. Camera self-calibration: Theory and experiments. In *Second European Conference on Computer Vision*, London, UK, 1992. Springer-Verlag.

[Ha, 2007] J.-E. Ha. Automatic detection of calibration markers on a chessboard. *Optical Engineering*, 46(10), 2007.

[Ha, 2009] J.-E. Ha. Automatic detection of chessboard and its applications. *Optical Engineering*, 48(6), 2009.

[Hartley, 1994] R. Hartley. Euclidean reconstruction from uncalibrated views. In *Second Joint European - US Workshop on Applications of Invariance in Computer Vision*, London, UK, 1994. Springer-Verlag.

[Luong and Faugeras, 1997] Q.-T. Luong and O.D. Faugeras. Self-calibration of a moving camera from point correspondences and fundamental matrices. *International Journal of Computer Vision*, 22, 1997.

[Nguyen *et al.*, 2007] V. Nguyen, S. Gächter, A. Martinelli, N. Tomatis, and R. Siegwart. A comparison of line extraction algorithms using 2D range data for indoor mobile robotics. *Autonomous Robots*, 23(2), 2007.

[Peynot and Kassir, 2010] T. Peynot and A. Kassir. Laser-camera data discrepancies and reliable perception in outdoor robotics. In *IEEE/RSJ International Conference on Intelligent Robots and Systems*, 2010.

[Peynot *et al.*, 2010] T. Peynot, S. Scheding, and S. Terho. The Marulan Data Sets: Multi-Sensor Perception in Natural Environment with Challenging Conditions. *International Journal of Robotics Research*, 29(13), 2010.

[Pollefeys, 1999] M. Pollefeys. *Self-calibration and metric 3D reconstruction from uncalibrated image sequences*. PhD thesis, ESAT-PSI, Katholieke Universiteit Leuven, 1999.

[Remondino and Fraser, 2006] F. Remondino and C. Fraser. Digital camera calibration methods: considerations and comparisons. In *International Archives of Photogrammetry, Remote Sensing and Spatial Information Sciences*, Dresden, Germany, 2006.

[Rufli *et al.*, 2008] M. Rufli, D. Scaramuzza, and R. Siegwart. Automatic detection of checkerboards on blurred and distorted images. In *IEEE/RSJ International Conference on Intelligent Robots and Systems*, 2008.

[Scaramuzza *et al.*, 2007] D. Scaramuzza, A. Harati, and R. Siegwart. Extrinsic self calibration of a camera and a 3D laser range finder from natural scenes. In *IEEE/RSJ International Conference on Intelligent Robots and Systems*, 2007.

[Scaramuzza, 2009] D. Scaramuzza. OCamCalib toolbox: Omnidirectional camera and calibration toolbox for matlab, 2009. `http://asl.epfl.ch/~scaramuz/research/Davide_Scaramuzza_files/Research/OcamCalib_Tutorial.htm`.

[Strobl *et al.*, 2009] K. Strobl, W. Sepp, S. Fuchs, C. Paredes, and K. Arbter. DLR CalLab and CalDe - The DLR Camera Calibration Toolbox, 2009. `http://www.dlr.de/rm/desktopdefault.aspx/tabid-4853/`.

[Vezhnevets, 2010] V. Vezhnevets. OpenCV and MatLab camera calibration toolboxes enhancement, 2010. `http://graphicon.ru/oldgr/en/research/calibration/index.html`.

[Wang *et al.*, 2010] Z. Wang, Z. Wang, and Y. Wu. Recognition of corners of planar pattern image. In *8th World Congress on Intelligent Control and Automation (WCICA)*, 2010.

[Zhang and Pless, 2004a] Q. Zhang and R. Pless. Constraints for heterogeneous sensor auto-calibration. In *Computer Vision and Pattern Recognition Workshop*, 2004.

[Zhang and Pless, 2004b] Q. Zhang and R. Pless. Extrinsic calibration of a camera and laser range finder (improves camera calibration). In *IEEE/RSJ International Conference on Intelligent Robots and Systems*, 2004.

[Zhou and Fang, 2010] D.-S. Zhou and X.-Y. Fang. Multi-chessboards localisation based on FCM and radon transform algorithm. *International Journal of Computer Applications in Technology*, 38, 2010.